JOURNAL OF THERMOPHYSICS AND HEAT TRANSFER
Vol. 23, No. 3, July–September 2009

Analytical Model of Ablation Using Bimodal Velocity Distribution Function in Knudsen Layer

L. Pekker*
ERC Inc., Edwards Air Force Base, California 93524

DOI: 10.2514/1.41255

An analytical model of the Knudsen layer at ablative surfaces has been developed that takes into account the temperature gradient in the bulk gas and rebound of gas particles by the ablative wall back into the gas region. This model uses a bimodal velocity distribution function, which preserves the laws of conservation of mass, momentum, and energy within the Knudsen layer and converges to the Chapman–Enskog velocity distribution function at the outer boundary of the Knudsen layer. The region of validity of this model and effects of the temperature gradient, diffusive reflection, and specular reflection on the Knudsen layer properties are calculated.

Nomenclature

a	=	index for the outer boundary of the Knudsen layer
b	=	index for the inner boundary of the Knudsen layer (for the wall)
B_V^τ, B_V^u, B_n^τ, B_n^u, B_β^τ, B_β^u	=	calculated constants
C_1	=	normalized flux of particles
C_2	=	normalized flux of momentum
C_3	=	normalized flux of energy multiplied by two
E_x	=	energy flux in x direction
f	=	velocity distribution function
F_{evap}	=	distribution function of evaporated particles
f_M	=	Maxwellian velocity distribution function
HK	=	index for Hertz–Knudsen variables
I	=	general functions
k	=	Boltzmann constant
m	=	mass of an ablated molecule
M_x	=	mass flux in x direction
n	=	gas number density
n_{sat}	=	equilibrium gas number density
n^*	=	number density of diffusively reflected particles
P_x	=	momentum flux in x direction
T	=	temperature
T_0	=	temperature of ablated surface
u	=	directed velocity
V_T	=	thermal gas velocity
V_x	=	x component of velocity
V_y	=	y component of velocity
V_z	=	z component of velocity
α	=	ratio of the directed velocity to the thermal velocity
β	=	general parameter
γ	=	accommodation coefficient, $\gamma = 1$ for specular and 0 for diffusive reflection
δa	=	parameter of the I integrals
δx_T	=	characteristic gradient length
$\delta(x)$	=	arbitrary function that satisfies the conditions $\delta(0) = 1$ and $\delta(\infty) = 1$
θ_c	=	condensation coefficient
λ_{mfp}	=	mean free path
ν	=	collision frequency
τ_T	=	thermal conduction parameter
Ψ, ω	=	condensation constant
$\uparrow$	=	index describing particles falling to the surface
$\downarrow$	=	index describing particles leaving the surface
$\hat{}$	=	index of normalization
$\bar{}$	=	index indicating the ratio of Hertz–Knudsen parameter to the corresponding modeled parameter

I. Introduction

ONE of the most important issues in computational fluid dynamics (CFD) modeling of ablation processes is the formulation of boundary conditions at the gas–surface interface. Generally, such boundary conditions cannot be obtained without analytical or parametric numerical modeling of the Knudsen layer formed near the ablated surface. Therefore, analytical models of the Knudsen layer are of interest for CFD simulations of ablative flows and have been widely used for a number of applications such as vaporization of liquids [1], capillary discharges [2,3], plasma thrusters [4,5], high-pressure discharges [6], vacuum arcs [7], electroguns [8], laser ablation [9], and others.

Anisimov [10] was the first to consider details of the vaporization process for a metal exposed to laser radiation. He used a bimodal velocity distribution function in the kinetic layer, assuming 1) there was no absorption of laser radiation in the ablated gas; 2) the gas flow velocity at the external boundary of the Knudsen layer is equal to the sound velocity; 3) the temperature of the gas in the equilibrium region (beyond the Knudsen layer, Fig. 1) is constant, that is, there is no conductive heat flux to the ablative wall surface; and 4) the condensation coefficient, defined as the ratio of incident molecules absorbed by the surface to those that hit the surface, was one, thus assuming that all particles that hit the ablative surface are absorbed by it. In the model, Anisimov used mass, momentum, and energy conservation laws to determine the parameter of his bimodal velocity distribution function in the Knudsen layer, thus modeling the collisions in the Knudsen layer. The primary result of his work was the calculation of the maximal flux of atoms returning to the evaporating surface, which was found to be about 18% of the flux of vaporized atoms. Ytrehus [11] has used the Anisimov [10] and his own bimodal velocity distribution functions in the Knudsen layer to study the effect of bulk gas pressure on downstream vapor flow. He has calculated the gas flow velocity at the external boundary of the Knudsen layer (in the bulk gas) as a function of the ratio of the equilibrium vapor pressure to the gas pressure in the bulk region. He

Presented as Paper 3910 at the 40th AIAA Thermophysics Conference, Double Tree Hotel Seattle Airport, Seattle, WA, 23–26 June 2008; received 30 September 2008; accepted for publication 17 February 2009.

*Research Scientist, 10 East Saturn Boulevard; leonid.pekker.ctr@edwards.af.mil.

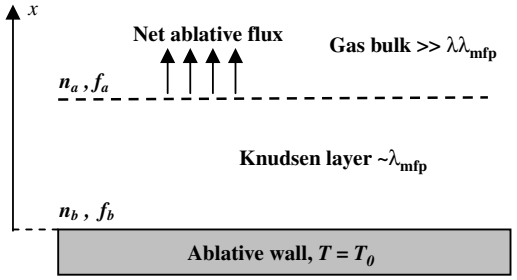

Fig. 1 Schematic representation of the layer structure near the ablative surface.

has demonstrated that the differences between the solutions using the Anisimov approximation and his own (more sophisticated) velocity distribution function are very small.

Later the Anisimov bimodal velocity distribution function was used in modeling the vaporization into dense plasmas. Beilis [12,13] applied this function to study the case of metal vaporization into discharge plasmas in a vacuum arc cathode spot and then Keidar et al. [14–16] for the case of ablation of dielectric walls in capillary discharges. All those analytical models neglected the conductive heat flux to the ablative surface. This can be significant because the temperature in the plasma core is assumed in the models to be much greater than the temperature of the ablative surface. Consequently, this results in a heat flux through the Knudsen layer being directed upward to the plasma chamber, Fig. 1, leading to an inconsistency in those models.

In the paper of Pekker et al. [17], the authors used a new bimodal velocity distribution function in the kinetic layer and built a more general Knudsen layer model, which takes into account the conductivity of the bulk gas. The main impetus of their paper was to study the effect of thermal conductivity on the Knudsen layer formed near the ablated surface. They have demonstrated that their model converges to the previous models [10,12–16] for the case where the external heat flux to the ablative surface becomes much larger then the conduction heat flux. This case corresponds to the situation where the external heat source heats only the ablative surface and not the gas (plasma) as, for example, in the case of laser ablation [10], where the externally applied laser radiation source heats only the ablating surface but for which the gas (plasma) is transparent. However, as in all other bimodal velocity distribution function models, the model in [17] has assumed that the condensation coefficient is equal to unity. This limits its applicability to many cases. For example, in water evaporation experiments, the measured condensation coefficient at some conditions can be very small, less than 0.1 [18,19]. The numerical calculations of the condensations coefficients can be found in [20,21].

We would like to point out the recent paper by Bond and Struchtrup [1] in which the authors have included the conduction heat flux in their analytical model of water evaporation. In that paper the authors have extended the classical collisionless Hertz–Knudsen model of the Knudsen layer [22,23] to the case of thermal conduction in the bulk gas, considered diffusive and specular reflections of particles, and allowed for nonflat wall–gas interfaces. However, their model ignores collisions in the Knudsen layer, and therefore the law of the conservation of momentum does not hold through the Knudsen layer. It should be stressed that the Hertz–Knudsen assumption of no collisions in the Knudsen layer is inconsistent because it assumes no "relaxation" in the kinetic (Knudsen) layer, whereas the velocity distribution function at the ablative surface has to relax (converge) to the bulk gas distribution function at the outer boundary of the given Knudsen layer.

Ideally Monte Carlo simulations or numerical solutions of the Bhatnar–Gross–Krook (BGK) equation describing the kinetic layer without any prior approximation of gas velocity distribution function in that layer should be able to self-consistently describe the conductive heat flux to the ablating surface. However, this will require extending the analysis beyond the Knudsen layer region, making it computationally intensive. As shown in [11,24–27], the models that use the Anisimov bimodal velocity distribution function, nevertheless, are in good agreement with the experimental finding, direct simulation Monte Carlo (DSMC), and numerical solutions of BGK equation. In the recent paper of Pekker et al. [28], the authors provided analysis of the applicability of a new bimodal velocity distribution function [17] through comparison of results with the solutions of the ellipsoidal statistical BGK (ES-BGK) model kinetic equation. They have demonstrated that the models are in good agreement and converge with a decrease in the Knudsen number.

Thus, improving the analytical models by including the process of rebounds of falling particles by the ablative surface back to the chamber is an important step in developing practical (computationally efficient) solutions for modeling of evaporation processes and plasma discharges coupled to ablative processes.

In this paper we develop an analytical evaporation (ablation) model, which extends the Knudsen layer model [17] to the case of arbitrary condensation and accommodation coefficients. The Knudsen layer model is presented in the next section. Numerical results and comparison of the presented model with the generalized collisionless Hertz–Knudsen model are presented in the Secs. III and IV, respectively. In Sec. V we briefly review the results and present conclusions.

II. Model

The following sections describe the assumptions and the model.

A. Gas Distribution Function at the Ablative Surfaces

When a particle in vapor phase hits the ablative wall (solid or liquid), it can be absorbed by the wall or rebounded back to the gas region. In general, the rebounded particle will exchange energy and momentum with "wall" particles. Thus, some knowledge about the absorption and reflection mechanisms is required. Following the commonly used simplified model, the absorption and rebound processes can be described by several coefficients.

The condensation coefficient θ_c is defined as the ratio of incident molecules absorbed by the surface to those that actually hit the surface. Thus, the case where all molecules that reach the surface of the wall are absorbed by the wall corresponds to $\theta_c = 1$, and the case of $\theta_c = 0$ corresponds to the opposite situation, that is, where all molecules are rebounded by the wall. Because a molecule hitting the wall with a higher normal velocity to the wall surface has a larger probability of being absorbed by the wall, Tsuruta et al. [29] suggested the condensation coefficient of the form

$$\theta_c = \psi \cdot \left[1 - \omega \cdot \exp\left(\frac{-V_x^2}{V_T^2}\right)\right] \tag{1}$$

where ψ and ω are constants, $T_0 = m \cdot V_T^2/(2 \cdot k)$ is the temperature of the ablated surface, m is the particle mass, and V_x is the particle velocity normal to the wall with the x axis directed from the wall to the gas chamber, as shown in Fig. 1.

To describe the reflection process we shall adopt the classical Maxwell model, which assumes that the molecules interact with the wall in two basic reflection mechanism: 1) specular, where the particle is reflected back to the chamber in a "mirrorlike" fashion, and 2) diffusive, where the reflected particle does not conserve its energy that it has before rebounding, but undergoes a completely thermal interaction with the surface and leaves the surface with the Maxwellian velocity function probability with the temperature equal to the wall surface temperature. To distinguish between specular and diffusive reflection, the commonly used accommodation coefficient γ is introduced, with $\gamma = 1$ for pure specular reflection and $\gamma = 0$ for pure diffusive reflection. For simplicity, we further assume that γ is constant, independent of velocity of the incident particle; this assumption is used in all previously developed models, see for example [1] and references therein.

The gas distribution function f_b at the wall can be written as

$$f_b = \begin{cases} f_{b\uparrow}(V_x, V_y, V_z) & V_x > 0 \\ f_{b\downarrow}(V_x, V_y, V_z) & V_x < 0 \end{cases} \tag{2}$$

$$n_b = \int_{-\infty}^{+\infty}\int_{-\infty}^{+\infty}\int_{-\infty}^{\infty} f_b(V_x, V_y, V_z)\cdot \mathrm{d}V_y \cdot \mathrm{d}V_z \cdot \mathrm{d}V_x \tag{3}$$

where $f_{b\downarrow}$ and $f_{b\uparrow}$ describe the particles falling to the ablative surface and leaving the surface, and n_b is the particle number density at the wall.

First let us consider the reflected particles. Following [1], the law of conservation of mass for reflected particles at the ablative surface can be written as

$$\begin{aligned} &\int_{-\infty}^{+\infty}\int_{-\infty}^{+\infty}\int_{-\infty}^{0}(1-\theta_c)\cdot V_x \cdot f_{b\downarrow}(V_x, V_y, V_z)\cdot \mathrm{d}V_y \cdot \mathrm{d}V_z \cdot \mathrm{d}V_x \\ &\quad + n^*\cdot(1-\gamma)\cdot \int_{-\infty}^{+\infty}\int_{-\infty}^{+\infty}\int_{0}^{\infty}(1-\theta_c)\cdot V_x \\ &\quad \cdot f_{M_b}(V_x, V_y, V_z, V_T)\cdot \mathrm{d}V_y \cdot \mathrm{d}V_z \cdot \mathrm{d}V_x \\ &\quad + \gamma \cdot \int_{-\infty}^{+\infty}\int_{-\infty}^{+\infty}\int_{0}^{\infty}(1-\theta_c)\cdot V_x \\ &\quad \cdot f_{b\downarrow}(-V_x, V_y, V_z)\cdot \mathrm{d}V_y \cdot \mathrm{d}V_z \cdot \mathrm{d}V_x = 0 \end{aligned} \tag{4}$$

where the first term is the flux of the particles that are reflected back to the chamber, the second and the third terms describe the diffusive and specular fluxes of the reflected particles, n^* and

$$f_{M_b} = \left(\frac{1}{\pi \cdot V_T^2}\right)^{3/2}\cdot \exp\left(-\frac{V_x^2+V_y^2+V_z^2}{V_T^2}\right) \tag{5}$$

are the number density and the velocity distribution function of diffusively reflected particles. Combining the first and the third terms in Eq. (4) we obtain

$$n^* = -\frac{\int_{-\infty}^{+\infty}\int_{-\infty}^{+\infty}\int_{-\infty}^{0}(1-\theta_c)\cdot V_x \cdot f_{b\downarrow}(V_x, V_y, V_z)\cdot \mathrm{d}V_y \cdot \mathrm{d}V_z \cdot \mathrm{d}V_x}{\int_{-\infty}^{+\infty}\int_{-\infty}^{+\infty}\int_{0}^{\infty}(1-\theta_c)\cdot V_x \cdot f_{M_b}(V_x, V_y, V_z, V_T)\cdot \mathrm{d}V_y \cdot \mathrm{d}V_z \cdot \mathrm{d}V_x} \tag{6}$$

Thus, the part of the gas distribution function describing the particles leaving the ablated surface can be written as

$$\begin{aligned} f_{b\uparrow} &= F_{\mathrm{evap}}(V_x, V_y, V_z) + n^*\cdot(1-\gamma)\cdot(1-\theta_c) \\ &\quad \cdot f_{M_b}(V_x, V_y, V_z, V_T) + \gamma\cdot(1-\theta_c)\cdot f_{b\downarrow}(-V_x, V_y, V_z) \end{aligned} \tag{7}$$

where F_{evap} is the distribution function of the evaporated particles. Let us obtain F_{evap} in thermodynamic equilibrium, where the gas distribution function at the ablated surface shall be Maxwellian with the equilibrium gas number density n_{sat} dependent on the wall surface temperature. Thus, in equilibrium, $n_b = n_{\mathrm{sat}}(T_0)$ and $f_b = n_{\mathrm{sat}}\cdot f_{M_b}$, and from Eqs. (6) and (7) we consequently obtain [1] that $n^* = n_{\mathrm{sat}}$ and

$$F_{\mathrm{evap}} = \theta_c \cdot n_{\mathrm{sat}} \cdot f_{M_b}(V_x, V_y, V_z, V_T) \tag{8}$$

Assuming that the nonequilibrium between the vapor and ablative surface has a negligible effect on the evaporation process, such as strong impacts of vapor particles that kick a wall particle out of the wall, we can use the vaporization function Eq. (5) in nonequilibrium conditions, too. This assumption is widely used in ablation and evaporation models, see for example [1,10–17]. Substituting Eqs. (7) and (8) into Eq. (2) we finally obtain

$$f_b = \begin{cases} [\theta_c \cdot n_{\mathrm{sat}} + n^*\cdot(1-\gamma) \\ \quad \cdot(1-\theta_c)]\cdot f_{M_b}(V_x, V_y, V_z, V_T) \\ \quad + \gamma\cdot(1-\theta_c)\cdot f_{b\downarrow}(-V_x, V_y, V_z) & V_x > 0 \\ f_{b\downarrow}(V_x, V_y, V_z) & V_x < 0 \end{cases} \tag{9}$$

where θ_c and n^* are given by Eqs. (1) and (6). Thus, the surface temperature of the wall, the condensation and accommodation coefficients, and the distribution function of incident particles at the wall $f_{b\downarrow}$ determine the gas distribution function at the ablative surface f_b; f_b is the gas distribution function at the inner boundary of the Knudsen layer, Fig. 1.

B. Bimodal Velocity Distribution Function in the Knudsen Layer

Following Anisimov's method [10,17] the velocity distribution function in the kinetic layer can be written in the following form, Fig. 1:

$$f(x, \mathbf{V}) = \delta(x)\cdot f_b(\mathbf{V}) + [1-\delta(x)]\cdot f_a(\mathbf{V}) \tag{10}$$

$$f_a(\mathbf{V}) = n_a \cdot f_{M_a}(\mathbf{V})\cdot\left\{1 - \frac{V_{T_a}}{\nu}\cdot\left[\frac{(V_x-u)}{V_{T_a}} \cdot\left(\frac{(V_x-u)^2+V_y^2+V_z^2}{V_{T_a}^2} - \frac{5}{2}\right)\cdot\frac{\mathrm{d}}{\mathrm{d}x}(\ln T_a)\right]\right\} \tag{11}$$

$$f_{M_a}(V_x, V_y, V_z, V_{T_a}, u) = \left(\frac{1}{\pi\cdot V_{T_a}^2}\right)^{3/2}\cdot\exp\left(-\frac{[(V_x-u)^2+V_y^2+V_z^2]}{V_{T_a}^2}\right) \tag{12}$$

where f_b is the gas distribution function at the inner boundary of the Knudsen layer given by Eq. (9) and f_a is the Chapman–Enskog velocity distribution function [30] at the outer boundary of the Knudsen layer that takes into account the temperature gradient and directed velocity above the Knudsen layer, in the gas bulk. Here n_a, u_a, V_{T_a}, and $T_a = m\cdot V_{T_a}^2/(2\cdot k)$ are the number density, directed velocity, thermal velocity, and temperature; ν is the collision frequency dependent on the temperature and density of the gas, $\mathrm{d}T_a/\mathrm{d}x$ is the gas bulk temperature gradient at the outer boundary of the Knudsen layer; $\delta(x)$ is an unknown function that satisfies the conditions $\delta(0) = 1$ and $\delta(\infty) = 0$. Substituting $f_{b\downarrow}$ into Eq. (9) in the form [10,17]

$$f_{b\downarrow}(\mathbf{V}) = \beta\cdot n_a \cdot f_{M_a}(V_x, V_y, V_z, V_{T_a}, u) \tag{13}$$

we complete the Knudsen layer model.

Normalizing all number densities by the equilibrium vapor density $n_{\mathrm{sat}}(T_0)$ and all velocities by V_T

$$\hat{n}^* = \frac{n^*}{n_{\mathrm{sat}}}, \qquad \hat{n}_a = \frac{n_a}{n_{\mathrm{sat}}}, \qquad \hat{V}_{T_a} = \frac{V_{T_a}}{V_T}$$
$$\hat{u} = \frac{u}{V_T}, \qquad \hat{T}_a = \frac{V_{T_a}^2}{V_T^2} \tag{14}$$

and then substituting Eqs. (5) and (13) into Eq. (6), we obtain the dimensionless system of equations for the Knudsen layer, which takes into account the thermal conductivity of the bulk gas and the specular and diffusive particle reflections from the ablative surfaces,

$$\hat{f}_b = \begin{cases} \left(\frac{1}{\sqrt{\pi}}\right)^3\cdot[\theta_c + \hat{n}^*\cdot(1-\gamma)\cdot(1-\theta_c)] \\ \quad \cdot\exp(-(\hat{V}_x^2+\hat{V}_y^2+\hat{V}_z^2)) + \gamma\cdot(1-\theta_c) \\ \quad \cdot\beta\cdot\hat{n}_a\cdot\left(\frac{1}{\sqrt{\pi}\cdot\hat{V}_{T_a}}\right)^3\exp\left(-\frac{(\hat{V}_x+\hat{u})^2+\hat{V}_y^2+\hat{V}_z^2}{\hat{V}_{T_a}^2}\right) & \hat{V}_x > 0 \\ \beta\cdot\hat{n}_a\cdot\left(\frac{1}{\sqrt{\pi}\cdot\hat{V}_{T_a}}\right)^3\cdot\exp\left(-\frac{(\hat{V}_x-\hat{u})^2+\hat{V}_y^2+\hat{V}_z^2}{\hat{V}_{T_a}^2}\right) & \hat{V}_x < 0 \end{cases} \tag{15}$$

$$\hat{f}_a = \hat{n}_a \cdot \left(\frac{1}{\sqrt{\pi}\cdot \hat{V}_{T_a}}\right)^3 \cdot \exp\left(-\frac{(\hat{V}_x-\hat{u})^2+\hat{V}_y^2+\hat{V}_z^2}{\hat{V}_{T_a}^2}\right) \cdot \left\{1-\frac{V_T\cdot \hat{V}_{T_a}}{\nu}\cdot\left[\frac{(\hat{V}_x-\hat{u})}{\hat{V}_{T_a}}\cdot\left(\frac{(\hat{V}_x-\hat{u})^2+\hat{V}_y^2+\hat{V}_z^2}{\hat{V}_{T_a}^2}-\frac{5}{2}\right)\cdot\frac{\mathrm{d}}{\mathrm{d}x}(\ell_n T_a)\right]\right\} \tag{16}$$

$$\theta_c = \psi\cdot[1-\omega\cdot\exp(-\hat{V}_x^2)] \tag{17}$$

$$\hat{n}^* = \beta\cdot\hat{n}_a\cdot\frac{[(1-\psi)\cdot I_{12}(\hat{V}_{T_a},\hat{u})+\psi\cdot\omega\cdot I_{13}(\hat{V}_{T_a},\hat{u})]}{((1-\psi)\cdot I_{10}+\psi\cdot\omega\cdot I_{11})} \tag{18}$$

The integrals I are given in Appendix A. It has to be mentioned that substituting the condensation coefficient equal to one ($\psi = 1$ and $\omega = 0$) into Eq. (15), we recover model [17], and assuming further no temperature gradient in the bulk gas, $\mathrm{d}(\ell_n T_a)/\mathrm{d}x = 0$ we obtain Anisimov's model [10].

Assuming the laws of conservation of mass, momentum, and energy hold at all times within the Knudsen layer, as it has been assumed in all previous models [10–17] (quasi-steady-state approximation within the Knudsen layer), the following integrals are defined [17]:

$$C_1 = \int_{-\infty}^{+\infty}\mathrm{d}V_z\int_{-\infty}^{\infty}\mathrm{d}V_y\int_{-\infty}^{+\infty} f\cdot V_x\cdot\mathrm{d}V_x = \hat{n}_a\cdot\hat{u} \tag{19}$$

$$C_2 = \int_{-\infty}^{+\infty}\mathrm{d}V_z\int_{-\infty}^{\infty}\mathrm{d}V_y\int_{-\infty}^{+\infty} f\cdot V_x^2\cdot\mathrm{d}V_x = \hat{n}_a\cdot\left(\hat{u}^2+\frac{\hat{V}_{T_a}^2}{2}\right) \tag{20}$$

$$C_3 = \int_{-\infty}^{+\infty}\mathrm{d}V_z\int_{-\infty}^{\infty}\mathrm{d}V_y\int_{-\infty}^{+\infty} f\cdot V^2\cdot V_x\cdot\mathrm{d}V_x = \hat{n}_a\cdot\left[\hat{u}\cdot\left(\hat{u}^2+\frac{5\cdot\hat{V}_{T_a}^2}{2}\right)-\frac{(V_T\cdot\hat{V}_{T_a})}{\nu}\cdot\frac{\mathrm{d}(\ell_n T_a)}{\mathrm{d}x}\cdot\frac{5\cdot\hat{V}_{T_a}^3}{4}\right] \tag{21}$$

where the values of C_1, C_2, and C_3 obtained at the outer boundary of the Knudsen layer (where δ is equal to zero), and the mass, momentum, and energy fluxes are

$$M_x = m\cdot n_{\mathrm{sat}}\cdot V_T\cdot C_1 \tag{22}$$

$$P_x = m\cdot n_{\mathrm{sat}}\cdot V_T^2\cdot C_2 \tag{23}$$

$$E_x = m\cdot n_{\mathrm{sat}}\cdot\frac{V_T^3}{2}\cdot C_3 \tag{24}$$

Here, E_x consists of the two parts: the conduction heat flux and the enthalpy flux of the gas moving with a directed velocity, Eq. (21). Taking into account that integrals C_1, C_2, and C_3 are preserved through the Knudsen layer and they should be independent of $\delta(x)$, we obtain the following equations corresponding to C_1, C_2, and C_3:

$$C_1 = [\psi+\hat{n}^*\cdot(1-\psi)]\cdot I_{10}-\psi\cdot\omega\cdot[1-\hat{n}^*]\cdot I_{11}-\beta\cdot\hat{n}_a\cdot I_{12}(\hat{V}_{T_a},\hat{u}) \tag{25}$$

$$C_2 = [\psi+\hat{n}^*\cdot(1-\gamma)\cdot(1-\psi)]\cdot I_{20}-\psi\cdot\omega\cdot[1-\hat{n}^*\cdot(1-\gamma)]\cdot I_{21}+[1+\gamma\cdot(1-\psi)]\cdot\beta\cdot\hat{n}_a\cdot I_{22}(\hat{V}_{T_a},\hat{u})+\gamma\cdot\psi\cdot\omega\cdot\beta\cdot\hat{n}_a\cdot I_{23}(\hat{V}_{T_a},\hat{u}) \tag{26}$$

$$C_3 = [\psi+\hat{n}^*\cdot(1-\gamma)\cdot(1-\psi)]\cdot I_{30}-\psi\cdot\omega\cdot[1-\hat{n}^*\cdot(1-\gamma)]\cdot I_{31}-[1-\gamma\cdot(1-\psi)]\cdot\beta\cdot\hat{n}_a\cdot I_{32}(\hat{V}_{T_a},\hat{u})+\gamma\cdot\psi\cdot\omega\cdot\beta\cdot\hat{n}_a\cdot I_{33}(\hat{V}_{T_a},\hat{u}) \tag{27}$$

with integral I given in Appendix A. It is worth noting again that particle flux through the kinetic layer C_1 for given $\hat{u}$, $\widehat{n}_a$, β, and $\widehat{V}_{T_a}$ is independent of γ because the mass flux is independent of how a particle is rebounded back to the gas by the wall, diffusively or specularly. In the case of $\omega = 0$, the condensation coefficient is independent of molecular velocity, the system of Eqs. (18) and (25–27) can be reduced to

$$\hat{n}^* = \beta\cdot\hat{n}_a\cdot\frac{I_{12}(\hat{V}_{T_a},\hat{u})}{I_{10}} \tag{28}$$

$$C_1 = [\psi+\hat{n}^*\cdot(1-\psi)]\cdot I_{10}-\beta\cdot\hat{n}_a\cdot I_{12}(\hat{V}_{T_a},\hat{u}) \tag{29}$$

$$C_2 = [\psi+\hat{n}^*\cdot(1-\gamma)\cdot(1-\psi)]\cdot I_{20}+[1+\gamma\cdot(1-\psi)]\cdot\beta\cdot\hat{n}_a\cdot I_{22}(\hat{V}_{T_a},\hat{u}) \tag{30}$$

$$C_3 = [\psi+\hat{n}^*\cdot(1-\gamma)\cdot(1-\psi)]\cdot I_{30}-[1-\gamma\cdot(1-\psi)]\cdot\beta\cdot\hat{n}_a\cdot I_{32}(\hat{V}_{T_a},\hat{u}) \tag{31}$$

This approximation, $\theta_c = \mathrm{const}$, is widely used in the literature [22,23,31–35]. It has to be stressed that Eq. (18) has an indeterminate form for the condensation coefficient equal to one ($\psi = 1$, $\omega = 0$) and, therefore, for this case Eqs. (28–31) must be used.

Following [17], let us introduce a thermal conduction parameter τ_T

$$\tau_T = \frac{V_T\cdot\hat{V}_{T_a}}{\nu}\cdot\frac{\mathrm{d}(\ell_n T_a)}{\mathrm{d}x}\approx\frac{\lambda_{\mathrm{mfp}}}{\delta x_T}\ll 1 \tag{32}$$

where $\lambda_{\mathrm{mfp}} = V_{T_a}/\nu$ is the characteristic gas mean free path at the outer boundary of the kinetic layer and $\delta x_T = [\mathrm{d}(\ell_n T_a)/\mathrm{d}x]^{-1}$ is the characteristic gradient length. The condition in Eq. (32) is needed for the Chapman–Enskog expansion method and Eq. (21) to be valid. Thus, our model is limited to relatively small values of the temperature gradients. It should be mentioned that in a recent paper [28] the authors demonstrated that the model [17], which is a special case of the present model with the condensation coefficient equal to one ($\psi = 1, \omega = 0$), is in good agreement with DSMC and numerical solution of ES-BGK model kinetic equations for the Knudsen number less than 0.2. In the future we are planning to investigate the applicability of our model for a wider region of Ψ, ω, and γ in a similar way as it has been done in [28].

In the case of small $\hat{u} \ll 1$ (small Mach numbers) Eqs. (18) and (25–27) can be further simplified to the following form:

$$\hat{V}_{T_a} = 1+\tau_T\cdot B_V^\tau+\widehat{u}\cdot B_V^u \tag{33}$$

$$\hat{n}_a = 1+\tau_T\cdot B_n^\tau+\widehat{u}\cdot B_n^u \tag{34}$$

$$\beta = 1+\tau_T\cdot B_\beta^\tau+\widehat{u}\cdot B_\beta^u \tag{35}$$

where

$$B_V^\tau = \frac{5\cdot\sqrt{\pi}}{8\cdot(1-\gamma+\gamma\cdot\psi)} \tag{36}$$

$$B_V^u = -\frac{\sqrt{\pi}\cdot(1+\gamma-\gamma\cdot\psi)}{8\cdot(1-\gamma+\gamma\cdot\psi)} \tag{37}$$

$$B_n^\tau = -\frac{5\cdot\sqrt{\pi}\cdot(3-\gamma+\gamma\cdot\psi)}{16\cdot(1-\gamma+\gamma\cdot\psi)} \tag{38}$$

$$B_n^u = -\sqrt{\pi}\cdot\left(\frac{32-27\cdot\psi-32\cdot\gamma+9\cdot\gamma^2\cdot\psi+46\cdot\gamma\cdot\psi-18\cdot\gamma^2\cdot\psi^2+9\cdot\gamma^2\cdot\psi^3-14\cdot\gamma\cdot\psi^2}{16\cdot(1-\gamma+\gamma\cdot\psi)\cdot\psi}\right)-\frac{4}{\sqrt{\pi}}\cdot\left(\frac{1+\gamma-\gamma\cdot\psi}{2}\right) \quad (39)$$

$$B_\beta^\tau = \frac{5\cdot\sqrt{\pi}}{16} \quad (40)$$

$$B_\beta^u = -\sqrt{\pi}\cdot\frac{9\cdot(1-\gamma^2+2\cdot\gamma^2\cdot\psi-\gamma^2\cdot\psi^2)}{16\cdot(1-\gamma+\gamma\cdot\psi)} + \frac{4}{\sqrt{\pi}}\cdot\left(\frac{1+\gamma-\gamma\cdot\psi}{2}\right) \quad (41)$$

The coefficients B have been obtained in Appendix B. As one can see, for $\hat{u}=0$ (in which case there is no ablation) and for $\tau_T>0$ (the conduction heat flux is directed from the chamber to the wall) the temperature and density at the outer edge of the Knudsen layer are correspondingly larger and smaller than one, Eqs. (36) and (38). These temperature and density jumps between the wall and Maxwellian gas at the outer boundary of the kinetic layer is a very well known phenomenon in gas dynamics, see for example [36]. Because the system of linear Eqs. (33–35) is much simpler than the systems of nonlinear Eqs. (18) and (25–27) and Eqs. (28–31)and does not need a sophisticated solver algorithm, it can be useful, for instance, for modeling of water or other liquid evaporation, where Knudsen layer model is part of a global evaporation model, and where typically the flow velocities are significantly smaller than the thermal velocity [1].

In the case of no ablation and no absorption of incident particles by the wall, $u=0$ and $\theta_c=0$, Eqs. (18) and (25–27) can be reduced to the following form:

$$n^* = \beta\cdot n_a\cdot\hat{V}_{T_a} \quad (42)$$

$$n_a\cdot\hat{V}_{T_a}^2 = n^*\cdot\frac{(1-\gamma)}{2}+(1+\gamma)\cdot\beta\cdot n_a\cdot\frac{\hat{V}_{T_a}^2}{2} \quad (43)$$

$$-n_a\cdot\tau_T\cdot\frac{5\cdot\hat{V}_{T_a}^3}{4} = n^*\cdot\frac{(1-\gamma)}{\sqrt{\pi}}-\beta\cdot\hat{n}_a\cdot\hat{V}_{T_a}^3\cdot\frac{(1-\gamma)}{\sqrt{\pi}} \quad (44)$$

where n^* and n_a correspond to the number density of diffusively reflected particles and the particle number density at the outer boundary of the Knudsen layer, respectively, Eqs. (6), (12), and (13) with $u=0$. Here Eqs. (43) and (44) correspond to the momentum and energy conservation laws, respectively, holding though the Knudsen layer; the mass conservation law is trivial, because the wall does neither evaporate nor absorb particles, only reflect incident particles. The particle number density at the inner boundary of the Knudsen layer can be obtained by integration of Eq. (9) with $f_{b\downarrow}$ from Eq. (13) with $u=0$, yielding

$$n_b = n^*\cdot\frac{(1-\gamma)}{2}+\gamma\cdot\beta\cdot n_a\cdot\frac{(1+\gamma)}{2} \quad (45)$$

Solving system of Eqs. (42–45) we can obtain

$$\hat{V}_{T_a} = \frac{\tau_T+(\tau_T^2+4\cdot(\frac{8}{5\cdot\sqrt{\pi}}-\frac{(1+\gamma)}{(1-\gamma)}\cdot\tau_T)\cdot\frac{8}{5\cdot\sqrt{\pi}})^{1/2}}{2\cdot(\frac{8}{5\cdot\sqrt{\pi}}-\frac{(1+\gamma)}{(1-\gamma)}\cdot\tau_T)} \quad (46)$$

$$\beta = -\tau_T\cdot\frac{5\cdot\hat{V}_{T_a}^2\cdot\sqrt{\pi}}{4\cdot(1-\gamma)\cdot(1-\hat{V}_{T_a}^2)} \quad (47)$$

$$\frac{n_b}{n_a} = \beta\cdot\left(\hat{V}_{T_a}\cdot\frac{(1-\gamma)}{2}+\frac{(\gamma+1)}{2}\right) \quad (48)$$

Because τ_T is assumed in the model to be much smaller than one, Eqs. (42) and (46–48) can be reduced to the following form:

$$\hat{V}_{T_a} = 1+\tau_T\cdot\frac{5\cdot\sqrt{\pi}}{8\cdot(1-\gamma)},\quad \beta = 1+\tau_T\cdot\frac{5\cdot\sqrt{\pi}}{16}$$
$$\frac{n_b}{n_a} = 1+\tau_T\cdot\frac{5\cdot\sqrt{\pi}}{8},\quad \frac{n^*}{n_a} = \left[1+\tau_T\cdot\frac{5\cdot\sqrt{\pi}\cdot(3-\gamma)}{16\cdot(1-\gamma)}\right] \quad (49)$$

As one can see, the expressions for $\hat{V}_{T_a}$ and β in Eq. (49) concur with corresponding Eqs. (33) and (35) at $\hat{u}=0$, and that has been expected. Because the normalized temperature jump for $\tau_T \ll 1$ is about two times larger than the normalized thermal velocity jump, Eq. (14), we obtain

$$\hat{T}_a = \frac{T_a}{T_0} = 1+\tau_T\cdot\frac{5\cdot\sqrt{\pi}}{4\cdot(1-\gamma)} \quad (50)$$

This equation can be used as a boundary conditions at a nonablative, nonabsorbing wall for modeling thermal conduction in gases [36]. For pure diffusive reflection $\gamma=0$ we obtain $\hat{T}_a \approx 1+\tau_T\cdot 2.2156$, which is closed to the data obtained by other authors [37].

III. Numerical Results

The effect of heat conduction in the case of an external heat flux to the ablative surface can be calculated, following [12–17], as a function of $\alpha = u/V_{Ta}$ for different τ_T, Eqs. (25–27). With an increase in the intensity of the external heat source that heats the ablative surface, not gas (plasma), the evaporation rate increases as do flow velocity and α. Thus, the distributions of the Knudsen layer parameters vs α for different values of τ_T (different thermal conduction heat fluxes) indeed represent the effect of heat conduction in the presence of an external ablative heat source.

Figure 2 shows the calculated parameters of the Knudsen layer for $\tau_T=0$, 0.1, and 0.2 at $\psi=0.5$, $\gamma=0$, and $\omega=0$. As one can see, with an increase in τ_T, the normalized temperature at the outer boundary of the Knudsen layer $\widehat{T}_a=\widehat{V}_{T_a}^2$ increases and the number density $\widehat{n}_a$ decreases; this agrees with [17], where similar calculations were performed for the case of a condensation coefficient equal to one. Figure 2 also illustrates the fact that with a decrease in τ_T (a decrease in thermal conduction) and increase in flow velocity or α (an increase in external heat flux to the ablative surface) the distributions of $\widehat{T}_a$ and $\widehat{n}_a$ converge to the case of $\tau_T=0$ [17]. It should be stressed that we cannot extend the results of Fig. 2 for larger τ_T because the Chapman–Enskog expansion method is valid only for $\tau_T \ll 1$.

Figure 3 shows the distributions of $\widehat{T}_a$ and $\widehat{n}_a$ and the normalized back flux of particles for different γ and $\tau_T=0.1$, $\psi=0.5$, and $\omega=0$. Here the back flux is the flux of the particle falling to the ablative surface and is given by $\beta\cdot\hat{n}_a\cdot I_{12}(\hat{V}_{T_a},\hat{u})$ [by the third term in Eq. (25)]. As we can see with an increase in α, the effect of γ on the

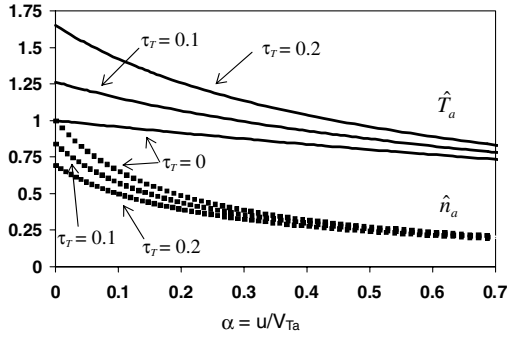

Fig. 2 Normalized parameters of the Knudsen layer for $\psi=0.5$, $\gamma=\omega=0$, and $\tau_T=0$, 0.1, and 0.2.

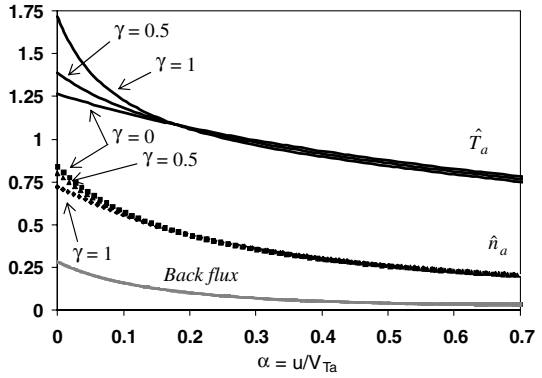

a)

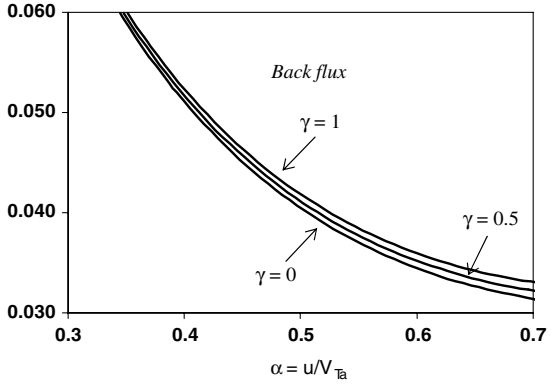

b)

Fig. 3 Normalized parameters of the Knudsen layer for $\tau_T = 0.1$, $\psi = 0.5$, $\omega = 0$, and $\gamma = 0$, 0.5, 1 showing a) temperatures and number densities at the outer boundary of the Knudsen layer and back fluxes, and b) zoomed distribution of the back fluxes.

temperature and density distributions becomes smaller. This makes perfect sense because with an increase in Mach number (or in α) the pure evaporation rate does not change, as shown in Eq. (8), whereas the back flux decreases as does the number of reflected particles, and, therefore, the parameters of the Knudsen layer become less dependent on γ, as particles are diffusively or specularly reflected. A tedious analytical analysis shows that the back flux for $\alpha = \omega = 0$ and $\psi = \text{const}$ is independent of γ. That is why the back flux in Fig. 3 shows week dependence on γ; with an increase in α the back fluxes diverge slightly, Fig. 3b.

Figure 4 shows the temperature and density distributions vs α calculated for different ψ and $\tau_T = 0.1$, $\gamma = \omega = 0$. The analysis shows that in this case of $\gamma = \omega = 0$, the $\widehat{T}_a$ and β are dependent on τ_T and α, and independent of ψ, whereas $\widehat{n}_a$ depends on all three parameters τ_T, α, and ψ, as can be seen in Fig. 4.

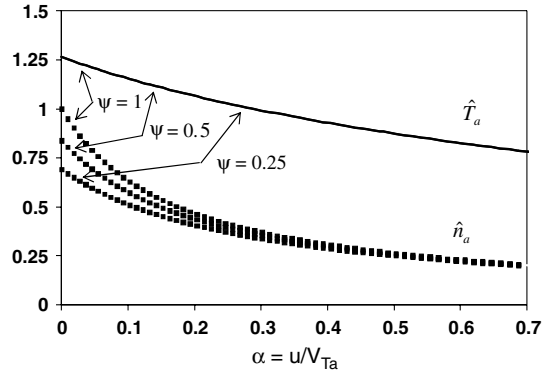

Fig. 4 Normalized parameters of the Knudsen layer for $\tau_T = 0.1$, $\gamma = \omega = 0$, and $\psi = 1$, 0.5, and 0.25.

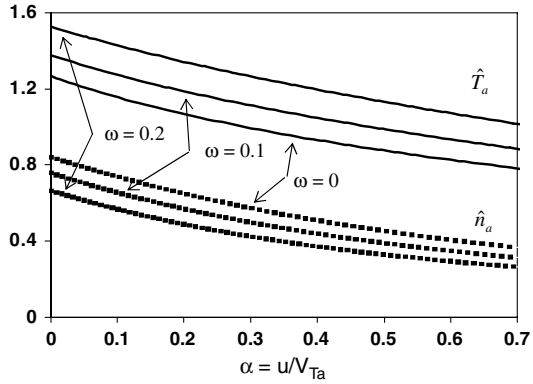

Fig. 5 Normalized parameters of the Knudsen layer for $\tau_T = 0.1$, $\psi = 1$, $\gamma = 0$, and $\omega = 0$, 0.1, 0.2.

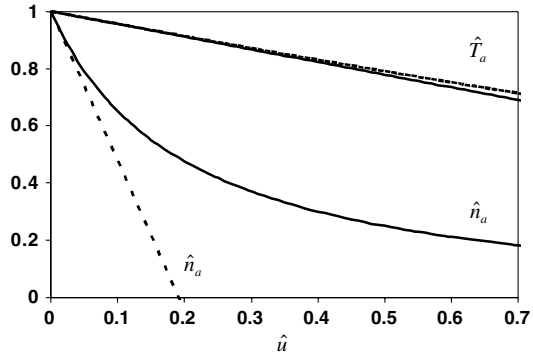

Fig. 6 Normalized parameters of the Knudsen layer for $\tau_T = 0$, $\psi = 0.5$, $\gamma = \omega = 0$; the general model, represented in Eqs. (18) and (25–27), are shown in the solid curves and the approximate model, represented in Eqs. (33–35), are shown in the dashed curves.

To investigate the effect of the microscopic condensation probability, seen in Eq. (1), on the macroscopic parameters of the Knudsen layer, we have calculated the distributions of $\widehat{T}_a$ and $\widehat{n}_a$ for different ω and $\tau_T = 0.1$, $\psi = 1$, and $\gamma = 0$, seen in Fig. 5. This figure shows that with an increase in ω, $\widehat{n}_a$ decreases. Again, this makes perfect sense because an increase in ω corresponds to an effective decrease in the condensation coefficient leading to a decrease in $\widehat{n}_a$, compare with Fig. 4. An increase in ω leads also to an increase in $\widehat{T}_a$, seen in Fig. 5, indicating that a dependence on the condensation coefficient of the velocity distribution function can significantly change the macroscopic parameters of the Knudsen layer.

To illustrate the restrictions for using the reduced model of the Knudsen layer, Eqs. (33–35), we have calculated the parameters of the Knudsen layer vs $\widehat{u}$ using both models: the original system of Eqs. (18) and (25–27) and the reduced system of Eqs. (33–35). Figure 6 shows the calculated distributions of $\widehat{T}_a$ and $\widehat{n}_a$ vs $\widehat{u}$ for $\tau_T = 0$, $\psi = 0.5$, $\omega = 0$, and $\gamma = 0$. As one can see, the difference between densities reaches almost 10% for $u = 0.05$. Thus, using the reduced system of equations for $\hat{u}$ larger than 0.05 is dangerous, particularly for small ψ and large γ, because the coefficient B_n^u increases as approximately ψ^{-1}, and B_V^τ, B_V^u, and B_n^τ as approximately $(1 - \gamma + \gamma \cdot \psi)^{-1}$, seen in Eqs. (36–39). However, it is worth noting that this reduced system of equations can be used for evaporation of liquid [1]. For example, it can be applied to model the evaporation of the ocean, where evaporation rates are so small that $\hat{u}$ is less than 0.05.

IV. Knudsen Layer Analytical Model

One commonly used analytical model of the Knudsen layer is the classical Hertz–Knudsen model [22,23], which assumes no collisions in the gas kinetic layer at the wall, the condensation

coefficient equal to one ($\psi = 1, \omega = 0$), and no thermal conductivity in the bulk gas. Bond and Struchtrup have shown [1] that in the case of nonzero thermal conduction to the wall, as long as the vapor is not too rarefied, the thermal conduction parameter $\tau_T \ll 1$, and the Mach number is small, $u \ll V_{T_a}$, the Chapmen–Enskog theory gives the same equations for mass and energy fluxes through the discontinuity region as does the classical Hertz–Knudsen theory

$$M_x = \frac{m \cdot n_{\text{sat}} \cdot V_T}{\sqrt{\pi}} - \frac{m \cdot n_a \cdot V_{T_a}}{\sqrt{\pi}} \tag{51}$$

$$E_x = \frac{m \cdot n_{\text{sat}} \cdot V_T^{3/2}}{\sqrt{\pi}} - \frac{m \cdot n_a \cdot V_{T_a}^{3/2}}{\sqrt{\pi}} \tag{52}$$

Moreover, Bond and Struchtrup have also generalized the Hertz–Knudsen theory to the case of the condensation coefficient given by Eq. (1) and considered diffusive and specular reflection, and nonflat wall–gas interfaces. However, their model, as well as the classical Knudsen layer model, ignores collisions in the Knudsen layer and, therefore, the law of conservation of momentum does not hold through the Knudsen layer. As mentioned in the Introduction, the Hertz-Knudsen assumption of no collisions in the Knudsen layer is inconsistent because it assumes no relaxation in the kinetic (Knudsen) layer, where the velocity distribution function at the ablative surface has to relax (converge) to the bulk gas distribution function at the outer boundary of the Knudsen given, in our case, by Eq. (11). That is why a comparison between a Hertz–Knudsen model and our model is important. Because our model as well as all others, including the Bond–Schruchtrup–Hertz–Knudsen model, gives the right asymptotical solution at thermodynamic equilibrium, where the mass and energy fluxes are equal to zero, we can expect differences in the Knudsen layer models in the region far from the equilibrium.

We can derive a Hertz–Knudsen model from our general model, Eqs. (18) and (25–27) by dropping the momentum conservation law equation, Eq. (26), and taking $\beta = 1$, literally using Eq. (15) with $\beta = 1$ for preserving the mass and energy conservation laws within the Knudsen layer

$$\hat{n}^* = \hat{n}_a \cdot \frac{[(1-\psi) \cdot I_{12}(\hat{V}_{T_a}, \hat{u}) + \psi \cdot \omega \cdot I_{13}(\hat{V}_{T_a}, \hat{u})]}{((1-\psi) \cdot I_{10} + \psi \cdot \omega \cdot I_{11})} \tag{53}$$

$$C_1 = [\psi + \hat{n}^* \cdot (1-\psi)] \cdot I_{10} - \psi \cdot \omega \cdot [1 - \hat{n}^*] \cdot I_{11} - \hat{n}_a \cdot I_{12}(\hat{V}_{T_a}, \hat{u}) \tag{54}$$

$$C_3 = [\psi + \hat{n}^* \cdot (1-\gamma) \cdot (1-\psi)] \cdot I_{30} - \psi \cdot \omega \cdot [1 - \hat{n}^* \cdot (1-\gamma)] \cdot I_{31} - [1 - \gamma \cdot (1-\psi)] \cdot \hat{n}_a \cdot I_{32}(\hat{V}_{T_a}, \hat{u}) + \gamma \cdot \psi \cdot \omega \cdot \hat{n}_a \cdot I_{33}(\hat{V}_{T_a}, \hat{u}) \tag{55}$$

Our generalized Hertz–Knudsen model differs from the Bond and Struchtrup model [1], where they have used first-order Taylor expansion of Eq. (11) about zero in α; thus, the Bond–Struchtrup model cannot be used for relatively large α.

Figure 7 represents a comparison of our general model, seen in Eqs. (18) and (25–27), and the Hertz–Knudsen model, seen in Eqs. (53–55), for $\tau_T = 0, 0.2$, $\psi = 0.5$, $\gamma = 0$, and $\omega = 0$, the case where half of the incident molecules are absorbed by the surface and half are diffusively rebounded back to the gas region. This figure shows the distributions of $\bar{T} = T_a^{\text{HK}}/T_a$ and $\bar{n} = n_a^{\text{HK}}/n_a$ vs α, where T_a^{HK} and n_a^{HK} are the temperature and number density at the outer boundary of the Knudsen layer calculated using the Hertz–Knudsen model. As one can see, in the case of no conduction heat ($\tau_T = 0$), the ratios $\bar{T}$ and $\bar{n}$ converge to unity as $\alpha \to 0$; this is expected because the case of $\tau_T = \alpha = 0$ corresponds to thermal equilibrium. However, with an increase in α (nonthermodynamic region) the temperature and density distributions calculated by the two models begin to diverge, and $|\bar{T} - 1|$ and $|\bar{n} - 1|$ for $\alpha = 0.7$ reach up to 5 and 10%, respectively. In the case of thermal conduction, with an increase in τ_T, the differences in the models rise: for $\tau_T = 0.2$ and $\alpha = 0$, the case of thermal heat conduction to the wall with no ablation, $|\bar{T} - 1|$ and $|\bar{n} - 1|$ reach 9 and 8%, respectively, and for $\tau_T = 0.2$ and $\alpha = 0.7$, 6 and 12%. Thus, it has been demonstrated that our model of the Knudsen layer gives very different results than the Hertz–Knudsen model.

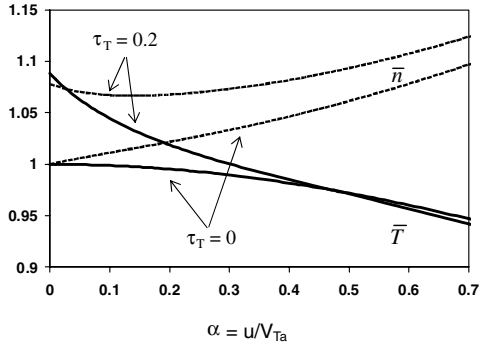

Fig. 7 Ratios o the Knudsen layer parameters at the outer boundary of the Knudsen layer calculated by the general model, represented in Eqs. (18) and (22–24), and by the Hertz–Knudsen generalized model, represented in Eqs. (41–43), for $\psi = 0.5$, $\gamma = \omega = 0$, and $\tau_T = 0$ and 0.2.

V. Conclusions

We presented an analytical model of the Knudsen layer near the ablative surface, taking into account the thermal conductivity in the adjusted bulk gas and the rebounding of particles from the ablative wall. This model employs a bimodal velocity distribution function, extending the previously developed Knudsen layer model [17] to the case of the sticking coefficient of incident particles to the ablative surface less than one. The model calculates the parameters of the Knudsen layer for the condensation coefficient given by Eq. (1) and an arbitrary accommodation coefficient. The gas mean free path at the outer boundary of the kinetic (Knudsen) layer in the model is assumed to be much smaller than the characteristic gradient length; this condition is needed for the Chapmen–Enskog expansion method to solve the Boltzmann equation used in the paper. Thus, this model is limited to relatively small temperature gradients. In the case of a larger temperature gradient, a more rigorous model is required, and only numerical simulation such as DSMC would solve the problem.

The widely used Hertz–Knudsen model and its generalizations assume no collisions in the Knudsen layer and, therefore, do not preserve the law of conservation of momentum within the Knudsen layer; they preserve only the mass and energy conservation laws. In comparison, our model preserves all three conservation laws. However, both models give the right asymptotical solution at thermodynamic equilibrium (where the mass and energy fluxes are equal to zero). That is why it was important to compare these models in cases that are far from thermodynamic equilibrium. Our calculations show significant differences between the two models. With an increase in the thermal conductive heating of the ablated surface or/and in the flow velocity, the differences between the two models dramatically increase; for $\tau_T = 0.2$, $\psi = 1$. $\omega = \gamma = 0$, and $\alpha = 0.7$ the differences in temperatures and density calculated at the outer boundary of the Knudsen layer reach up to almost 20%.

Ideally Monte Carlo simulation or numerical solutions of the Boltzmann equations should be able to self-consistently describe the conductive heat flux to the ablative surface without any prior approximation of the gas velocity distribution function in the kinetic layer. However, this will require extending the analysis beyond the Knudsen layer region, making it computationally intensive. Thus, our analytical model taking into account heat conduction, molecular condensation, and accommodation processes is an important step in developing practical (computationally efficient) solutions to the

problem of modeling evaporation processes and plasma discharges coupled to the ablative surface.

To the best of our knowledge, currently there is no experimental data that can allow direct experimental verification of the model, and comparison with direct simulation such as DSMC or BGK simulation will pay a verification role until a more complete physical model can be developed.

Appendix A: Integrals for Eqs. (18) and (25–27)

$$I_{10} = \frac{1}{\sqrt{\pi}} \cdot \int_0^\infty x \cdot \exp(-x^2) \cdot \mathrm{d}x = \frac{1}{2 \cdot \sqrt{\pi}} \tag{A1}$$

$$I_{20} = \frac{1}{\sqrt{\pi}} \cdot \int_0^\infty x^2 \cdot \exp(-x^2) \cdot \mathrm{d}x = \frac{1}{4} \tag{A2}$$

$$I_{30} = \left(\frac{1}{\sqrt{\pi}}\right)^3 \cdot \int_{-\infty}^\infty \mathrm{d}y \cdot \int_{-\infty}^\infty \mathrm{d}z \cdot \int_0^\infty x \cdot (x^2 + y^2 + z^2) \cdot \exp(-(x^2 + y^2 + z^2)) \cdot \mathrm{d}x = \frac{1}{\sqrt{\pi}} \tag{A3}$$

$$I_{11} = \frac{1}{\sqrt{\pi}} \cdot \int_0^\infty x \cdot \exp(-2x^2) \cdot \mathrm{d}x = \frac{1}{4 \cdot \sqrt{\pi}} \tag{A4}$$

$$I_{21} = \frac{1}{\sqrt{\pi}} \cdot \int_0^\infty x^2 \cdot \exp(-2x^2) \cdot \mathrm{d}x = \frac{1}{8 \cdot \sqrt{2}} \tag{A5}$$

$$I_{31} = \left(\frac{1}{\sqrt{\pi}}\right)^3 \cdot \int_{-\infty}^\infty \mathrm{d}y \cdot \int_{-\infty}^\infty \mathrm{d}z \cdot \int_0^\infty x \cdot (x^2 + y^2 + z^2) \cdot \exp(-(2x^2 + y^2 + z^2)) \cdot \mathrm{d}x = \frac{3}{8 \cdot \sqrt{\pi}} \tag{A6}$$

$$I_{12}(a,u) = \frac{1}{a \cdot \sqrt{\pi}} \cdot \int_0^\infty x \cdot \exp\left(-\frac{(x+u)^2}{a^2}\right) \cdot \mathrm{d}x = \frac{a}{2 \cdot \sqrt{\pi}} \cdot \left(\exp\left(-\frac{u^2}{a^2}\right) - \frac{u}{a} \cdot \sqrt{\pi} \cdot erfc\left(\frac{u}{a}\right)\right) \tag{A7}$$

$$I_{22}(a,u) = \frac{1}{a \cdot \sqrt{\pi}} \cdot \int_0^\infty x^2 \cdot \exp\left(-\frac{(x+u)^2}{a^2}\right) \cdot \mathrm{d}x = \frac{a^2}{4 \cdot \sqrt{\pi}} \cdot \left(-2 \cdot \frac{u}{a} \cdot \exp\left(-\frac{u^2}{a^2}\right) + \sqrt{\pi} \cdot \left(1 + 2 \cdot \frac{u^2}{a^2}\right) \cdot Erfc\left(\frac{u}{a}\right)\right) \tag{A8}$$

$$I_{32}(a,u) = \left(\frac{1}{a \cdot \sqrt{\pi}}\right)^3 \cdot \int_{-\infty}^\infty \mathrm{d}y \cdot \int_{-\infty}^\infty \mathrm{d}z \cdot \int_0^\infty x \cdot (x^2 + y^2 + z^2) \cdot \exp\left(-\frac{(x+u)^2 + y^2 + z^2}{a^2}\right) \cdot \mathrm{d}x = \frac{a^3}{4} \cdot \left(\frac{2}{\sqrt{\pi}} \cdot \exp\left(-\frac{u^2}{a^2}\right) \cdot \left(2 + \frac{u^2}{a^2}\right) - \frac{u}{a} \cdot \left(5 + 2 \cdot \frac{u^2}{a^2}\right) \cdot erfc\left(\frac{u}{a}\right)\right) \tag{A9}$$

$$I_{13}(a,u) = \frac{1}{a \cdot \sqrt{\pi}} \cdot \int_0^\infty x \cdot \exp\left(-\frac{(x+u)^2}{a^2} - x^2\right) \cdot \mathrm{d}x = \frac{1}{\sqrt{\pi}} \cdot \frac{a}{2 \cdot (1+a^2)} \cdot \left(\exp\left(-\frac{u^2}{a^2}\right) - \frac{u \cdot \sqrt{\pi}}{a \cdot \sqrt{a^2+1}} \cdot \exp\left(-\frac{u^2}{1+a^2}\right) \cdot erfc\left(\frac{u}{a \cdot \sqrt{a^2+1}}\right)\right) \tag{A10}$$

$$I_{23}(a,u) = \frac{1}{a \cdot \sqrt{\pi}} \cdot \int_0^\infty x^2 \cdot \exp\left(-\frac{(x+u)^2}{a^2} - x^2\right) \cdot \mathrm{d}x = \frac{1}{\sqrt{\pi}} \cdot \frac{a^2}{4 \cdot (1+a^2)^2} \cdot \left(-2 \cdot \frac{u}{a} \cdot \exp\left(-\frac{u^2}{a^2}\right) + \sqrt{\pi} \cdot \left(\sqrt{1+a^2} + 2 \cdot \frac{u^2}{a^2 \cdot \sqrt{1+a^2}}\right) \cdot \exp\left(-\frac{u^2}{1+a^2}\right) \cdot erfc\left(\frac{u}{a \cdot \sqrt{1+a^2}}\right)\right) \tag{A11}$$

$$I_{33}(a,u) = \left(\frac{1}{a \cdot \sqrt{\pi}}\right)^3 \cdot \int_{-\infty}^\infty \mathrm{d}y \cdot \int_{-\infty}^\infty \mathrm{d}z \cdot \int_0^\infty x \cdot (x^2 + y^2 + z^2) \cdot \exp\left(-\frac{(x+u)^2 + y^2 + z^2}{a^2} - x^2\right) \cdot \mathrm{d}x = \frac{1}{\sqrt{\pi}} \cdot \frac{a^3}{4 \cdot (1+a^2)^3} \cdot \left[\exp\left(-\frac{u^2}{a^2}\right) \cdot \left(4 + 2 \cdot a^4 + 6 \cdot a^2 + \frac{2 \cdot u^2}{a^2}\right) - \frac{u \cdot \sqrt{\pi}}{a \cdot \sqrt{1+a^2}} \cdot \exp\left(-\frac{u^2}{1+a^2}\right) \cdot \left(\frac{2 \cdot u^2}{a^2} + 5 + 7 \cdot a^2 + 2 \cdot a^4\right) \times erfc\left(\frac{u}{a \cdot \sqrt{1+a^2}}\right)\right] \tag{A12}$$

Appendix B: Derivations of the Coefficients for Eqs. (33–35)

Substituting $\alpha = 1 + \delta\alpha$ into Eqs. (A8–A12) and assuming u, $\delta\alpha \ll 1$ we obtain

$$J_{12}(\delta a, u) = \frac{1}{2 \cdot \sqrt{\pi}} \cdot (1 + \delta a - u \cdot \sqrt{\pi}) \tag{B1}$$

$$J_{22}(\delta a, u) = \frac{1}{4} \cdot \left(1 + 2 \cdot \delta a - \frac{4 \cdot u}{\sqrt{\pi}}\right) \tag{B2}$$

$$J_{32}(\delta a, u) = \frac{1}{\sqrt{\pi}} \cdot \left(1 + 3 \cdot \delta a - \frac{5 \cdot \sqrt{\pi}}{4} \cdot u\right) \tag{B3}$$

$$J_{13}(\delta a, u) = \frac{1}{4 \cdot \sqrt{\pi}} \cdot \left(1 - u \cdot \frac{\sqrt{\pi}}{\sqrt{2}}\right) \tag{B4}$$

$$J_{23}(\delta a, u) = \frac{\sqrt{2}}{16} \cdot \left(1 + \frac{\delta a}{2} - \frac{4 \cdot u}{\sqrt{2 \cdot \pi}}\right) \tag{B5}$$

$$J_{33}(\delta a, u) = \frac{1}{\sqrt{\pi}} \cdot \frac{3}{8} \cdot \left[1 + \frac{5}{3} \cdot \delta a - \frac{7 \cdot \sqrt{2 \cdot \pi}}{12} \cdot u\right] \tag{B6}$$

where functions $J_k(\delta\alpha, u)$ are the expansions of corresponding functions $I_k(\alpha, u)$ to first order in $\delta\alpha$ and u. Substituting I_{10}, I_{20}, and I_{30} from Eqs. (A1–A3) into Eqs. (28–31) and then using functions J_{12}, J_{22}, and J_{32}, Eqs. (B1–B3), instead of functions I_{12}, I_{22}, and I_{32} with

$$\hat{n}_a = 1 + \delta\hat{n}_a, \qquad \hat{V}_{T_a} = 1 + \delta\hat{V}_{T_a}, \qquad \beta = 1 + \delta\beta \tag{B7}$$

where $\delta\hat{n}_a$, $\delta\hat{V}_{T_a}$, $\delta\beta$, u, and τ_T are assumed to be much smaller than one, and after some tedious algebra, we obtain

$$\hat{n}^* = 1 + \delta\beta + \delta\hat{n}_a + \delta\hat{V}_{T_a} - u \cdot \sqrt{\pi} \tag{B8}$$

$$\hat{u} \cdot \sqrt{\pi} \cdot (2 - \psi) + \psi \cdot (\delta\beta + \delta\hat{n}_a + \delta\hat{V}_{T_a}) = 0 \tag{B9}$$

$$\delta\beta - \delta\hat{n}_a \cdot \left(\frac{\psi}{2-\psi}\right) - \delta\hat{V}_{T_a} \cdot \left(\frac{1-\gamma+\psi+\gamma\cdot\psi}{2-\psi}\right) - \hat{u} \cdot \left(\sqrt{\pi} \cdot \left(\frac{(1-\gamma)\cdot(1-\psi)}{2-\psi}\right) + \frac{4}{\sqrt{\pi}} \cdot \left(\frac{1+\gamma\cdot(1-\psi)}{2-\psi}\right)\right) = 0 \tag{B10}$$

$$\frac{5}{4} \cdot \tau_T - (\delta\hat{n}_a + \delta\beta) \cdot \frac{\psi}{\sqrt{\pi}} - \delta\hat{V}_{T_a} \cdot \left(\frac{2+\psi-2\cdot\gamma+2\cdot\gamma\cdot\psi}{\sqrt{\pi}}\right) - \hat{u} \cdot \left(\frac{9+\gamma-4\cdot\psi-\gamma\cdot\psi}{4}\right) = 0 \tag{B11}$$

The solution of this system of equation can be presented in the following form:

$$\hat{V}_{T_a} = 1 + \tau_T \cdot B_V^\tau + u \cdot B_V^u \tag{B12}$$

$$\hat{n}_a = 1 + \tau_T \cdot B_n^\tau + \hat{u} \cdot B_n^u \tag{B13}$$

$$\beta = 1 + \tau_T \cdot B_\beta^\tau + u \cdot B_\beta^u \tag{B14}$$

where

$$B_V^\tau = \frac{5 \cdot \sqrt{\pi}}{8 \cdot (1 - \gamma + \gamma \cdot \psi)} \tag{B15}$$

$$B_V^u = -\frac{\sqrt{\pi} \cdot (1 + \gamma - \gamma \cdot \psi)}{8 \cdot (1 - \gamma + \gamma \cdot \psi)} \tag{B16}$$

$$B_n^\tau = -\frac{5 \cdot \sqrt{\pi} \cdot (3 - \gamma + \gamma \cdot \psi)}{16 \cdot (1 - \gamma + \gamma \cdot \psi)} \tag{B17}$$

$$B_n^u = -\sqrt{\pi} \cdot \left(\frac{32 - 27\cdot\psi - 32\cdot\gamma + 9\cdot\gamma^2\cdot\psi + 46\cdot\gamma\cdot\psi - 18\cdot\gamma^2\cdot\psi^2 + 9\cdot\gamma^2\cdot\psi^3 - 14\cdot\gamma\cdot\psi^2}{16\cdot(1-\gamma+\gamma\cdot\psi)\cdot\psi}\right) - \frac{4}{\sqrt{\pi}} \cdot \left(\frac{1+\gamma-\gamma\cdot\psi}{2}\right) \tag{B18}$$

$$B_\beta^\tau = \frac{5 \cdot \sqrt{\pi}}{16} \tag{B19}$$

$$B_\beta^u = -\sqrt{\pi} \cdot \frac{9 \cdot (1 - \gamma^2 + 2 \cdot \gamma^2 \cdot \psi - \gamma^2 \cdot \psi^2)}{16 \cdot (1 - \gamma + \gamma \cdot \psi)} + \frac{4}{\sqrt{\pi}} \cdot \left(\frac{1 + \gamma - \gamma \cdot \psi}{2}\right) \tag{B20}$$

Coefficients B_i^j can be obtained in a similar way for a general case where $\omega \neq 0$, Eq. (1).

Acknowledgments

The author would like to express his appreciation to J.-L. Cambier for his encouragements to extend the Knudsen layer model to the case of arbitrary condensation and accommodation coefficients and his gratitude to A. Pekker for his kind help in preparing the text of this paper.

References

[1] Bond, M., and Struchtrup, H., "Mean Evaporation and Condensation Coefficients Based on Energy Dependent Condensation Probability," *Physical Review E (Statistical Physics, Plasmas, Fluids, and Related Interdisciplinary Topics)*, Vol. 70, No. 6, 2004, pp. 061605. doi:10.1103/PhysRevE.70.061605

[2] Seeger, M., Niemeyer, L., Christen, T., Schwinne, M., and Dommerque, R. J., "An Integral Arc Model for Ablation Controlled Arcs Based on CFD Simulations," *Journal of Physics D: Applied Physics*, Vol. 39, No. 10, 2006, pp. 2180–2191. doi:10.1088/0022-3727/39/10/029

[3] Keidar, M., and Beilis, I. I., "Nonequilibrium Thermal Boundary Layer in a Capillary Discharge with an Ablative Wall," *Physics of Plasmas*, Vol. 13, 2006, pp. 114503. doi:10.1063/1.2388953

[4] Burton, R., and Turchi, P., "Pulsed Plasma Thruster," *Journal of Propulsion and Power*, Vol. 14, No. 5, 1998, pp. 716–735. doi:10.2514/2.5334

[5] Keidar, M., Boyd, I. D., and Beilis, I. I., "Electrical Discharge in the Teflon Cavity of a Coaxial Pulsed Plasma Thruster," *IEEE Transactions on Plasma Sciences*, Vol. 28, No. 2, 2000, pp. 376–385. doi:10.1109/27.848096

[6] Boulos, M. I., Fauchais, P., and Pfender, E., *Thermal Plasmas: Fundamentals and Applications*, Plenum, New York, Vol. 1, 1995.

[7] Beilis, I. I., "Kinetic of Plasma Particles and Electron Transport in the Current-Carrying Plasma Adjacent to an Evaporating and Electron Emitting Wall," *IEEE Transactions on Plasma Sciences*, Vol. 34, No 3, 2006, pp. 885–866.

[8] Raja, L. L., Varghese, P. L., and Wilson, D. E., "Modeling of the Electrogun Metal Vapor Plasma Discharge," *Journal of Thermophysics and Heat Transfer*, Vol. 11, No. 3, 1997, pp. 353–360. doi:10.2514/2.6273

[9] Zhigilei, L. V., Kodali, P. B. D., and Garrison, B. J., "A Microscopic View of Laser Ablation," *Journal of Physical Chemistry B*, Vol. 102, No. 16, 1998, pp. 2845–2853. doi:10.1021/jp9733781

[10] Anisimov, S. I., "Vaporization of Metal Absorbing Laser Radiation," *Soviet Physics, JETP*, Vol. 27, No. 1, 1968, pp. 182–183.

[11] Ytrehus, T., "Theory and Experiments on Gas Kinetics in Evaporation," *Rarefied Gas Dynamics*, Vol. 51, AIAA, New York, 1976, pp. 1197–1213.

[12] Beilis, I. I, "Parameters of the Kinetic Layer of Arc-Discharge Cathode Region," *IEEE Transactions on Plasma Sciences*, Vol. 13, No. 5, 1985, pp. 288–290. doi:10.1109/TPS.1985.4316422

[13] Beilis, I. I, *Vacuum Arc Science and Technology*, edited by R. L. Boxman, P. Martin, D. Sanders, Noyes, Park Ridge, NJ, 2008.

[14] Keidar, M., Fan, J., Boyd, I. D., and Beilis, I. I., "Vaporization of Heated Materials into Discharge Plasmas," *Journal of Applied Physics*, Vol. 89, No. 6, 2001, pp. 3095–3098. doi:10.1063/1.1345860

[15] Keidar, M., Boyd, I. D., and Beilis, I. I., "On the Model of Teflon Ablation in an Ablation-Controlled Discharge," *Journal of Physics D: Applied Physics*, Vol. 34, No. 11, 2001, pp. 1675–1677. doi:10.1088/0022-3727/34/11/318

[16] Keidar, M., Boyd, I. D., and Beilis, I. I., "Ionization and Ablation Phenomena in an Ablative Plasma Accelerator," *Journal of Applied Physics*, Vol. 96, No. 10, 2004, pp. 5420–5428. doi:10.1063/1.1805726

[17] Pekker, L., Keidar, M., and Cambier, J.-L., "Effect of Thermal Conductivity on the Knudsen Layer at Ablative Surfaces," *Journal of Applied Physics*, Vol. 103, 2008, pp. 034906. doi:10.1063/1.2838210

[18] Eames, I. W, Marr, N. J, and Sabir, H., "The Evaporation Coefficient of Water: A Review," *International Journal of Heat and Mass Transfer*, Vol. 40, No. 12, 1997, pp. 2963–2973. doi:10.1016/S0017-9310(96)00339-0

[19] Marec, R., and Straub, J., "Analysis of the Evaporation Coefficient and the Condensation Coefficient of Water," *International Journal of Heat and Mass Transfer*, Vol. 44, No. 1, 2001, pp. 39–53. doi:10.1016/S0017-9310(00)00086-7

[20] Nagayama, G., and Tsuruta, T., "A General Expression for the Condensation Coefficient Based on Transition State and Molecular Dynamics Simulation," *Journal of Chemical Physics*, Vol. 118, No. 3, 2003, pp. 1392–1399.
doi:10.1063/1.1528192

[21] Meland, R., Frezzotti, A., Ytrehus, T., and Hafskjold, B., "Nonequilibrium Molecular-Dynamics Simulation of Net Evaporation and Net Condensation, and Evaluation of the Gas-Kinetic Boundary Condition at the Interphase," *Physics of Fluids*, Vol. 16, No. 2, 2004, pp. 223–243.
doi:10.1063/1.1630797

[22] Hertz, H., "Over the Evaporation of the Fluids, Especially the Mercury, in the Air Empty Room," *Annalen der Physik (Leipzig)*, Vol. 253, No. 10, 1882, pp. 177–193.
doi:10.1002/andp.18822531002

[23] Knudsen, M., "The Maximum Evaporation Speed of the Mercury," *Annalen der Physik (Leipzig)*, Vol. 352, No. 13, 1915, pp. 697–708.
doi:10.1002/andp.19153521306

[24] Sibold, D., and Urbassek, H. M., "Kinetic Study of Pulsed Desorption Flows into Vacuum," *Physical Review A*, Vol. 43, No. 12, 1991, pp. 6722–6734.
doi:10.1103/PhysRevA.43.6722

[25] Sibold, D., and Urbassek, H. M., "Monte Carlo Study of the Knudsen Layers in Evaporation from Elemental and Binary Media," *Physics of Fluids A*, Vol. 5, No. 1, 1993, pp. 243–256.
doi:10.1063/1.858779

[26] Morozov, A. A., "Thermal Model of Pulsed Laser: Back Flux Contribution," *Applied Physics A: Materials Science & Processing*, Vol. 79, Nos. 4–6, 2004, pp. 997–999.
doi:10.1007/s00339-004-2613-2

[27] Rose, J. W., "Accurate Approximation Equations for Intensive Sub-Sonic Evaporation," *International Journal of Heat and Mass Transfer*, Vol. 43, No. 20, 2000, pp. 3869–3875.
doi:10.1016/S0017-9310(00)00018-1

[28] Pekker, L., Gimelshein, N., and Gimelshein, S., "Analytical and Kinetic Modeling of Ablation Process,"*40th AIAA Thermophysics Conference*, AIAA 2007-3803, Seattle, WA, June 2008.

[29] Tsuruta, T., Tanaka, H., and Masuoka, T., "Condensation/Evaporation Coefficient and Velocity Distribution at Liquid-Vapor Interface," *International Journal of Heat and Mass Transfer*, Vol. 42, No. 22, 1999, pp. 4107–4116.
doi:10.1016/S0017-9310(99)00081-2

[30] Vincenti, W. G., and Kruger, C. H., Jr., "*Introduction to Physical Gas Dynamics*," Krieger, Malabar, FL, 1975.

[31] Pao, Y. P., "Application of Kinetic Theory to the Problem of Evaporation and Condensation," *Physics of Fluids*, Vol. 14, No. 2, 1971, pp. 306–312.
doi:10.1063/1.1693429

[32] Pao, Y. P., "Temperature and Density Jumps in the Kinetic Theory of Gases and Vapors," *Physics of Fluids*, Vol. 16, No. 9, 1973, pp. 1340–1346.
doi:10.1063/1.1694569

[33] Sone, Y., and Onishi, Y., "Kinetic Theory of Evaporation and Condensation, Hydrodynamic Equation and Slip Boundary Condition," *Journal of the Physical Society of Japan*, Vol. 44, No. 6, 1978, 1981–1994.
doi:10.1143/JPSJ.44.1981

[34] Young, J. B., "The Condensation and Evaporation of Liquid Droplets in a Pure Vapor at Arbitrary Knudsen Number," *International Journal of Heat and Mass Transfer*, Vol. 34, No. 7, 1991, pp. 1649–1661.
doi:10.1016/0017-9310(91)90143-3

[35] Sone, Y., *Kinetic Theory and Fluid Dynamics*, Birkhäuser, Boston, 2000.

[36] Kennard, E. H., *Kinetic Theory of Gases*, McGaw–Hill Book, New York, 1938.

[37] Sharipov, F., "Data on the Velocity Slip and Temperature Jump Coefficients," *Proceedings of the 5th International Conference on Thermal and Mechanical Simulation and Experiments in Microelectronics and Microsystems*, Brussels, 2004, pp. 243–249.